AUTISM

Exogenous and evoked oxytocin restores social behavior in the *Cntnap2* mouse model of autism

Olga Peñagarikano,[1,2] María T. Lázaro,[1] Xiao-Hong Lu,[3] Aaron Gordon,[4] Hongmei Dong,[1] Hoa A. Lam,[5] Elior Peles,[4] Nigel T. Maidment,[5] Niall P. Murphy,[5] X. William Yang,[3] Peyman Golshani,[1,6,7] Daniel H. Geschwind[1,2,3]*

Mouse models of neuropsychiatric diseases provide a platform for mechanistic understanding and development of new therapies. We previously demonstrated that knockout of the mouse homolog of *CNTNAP2* (contactin-associated protein-like 2), in which mutations cause cortical dysplasia and focal epilepsy (CDFE) syndrome, displays many features that parallel those of the human disorder. Because CDFE has high penetrance for autism spectrum disorder (ASD), we performed an in vivo screen for drugs that ameliorate abnormal social behavior in *Cntnap2* mutant mice and found that acute administration of the neuropeptide oxytocin improved social deficits. We found a decrease in the number of oxytocin immunoreactive neurons in the paraventricular nucleus (PVN) of the hypothalamus in mutant mice and an overall decrease in brain oxytocin levels. Administration of a selective melanocortin receptor 4 agonist, which causes endogenous oxytocin release, also acutely rescued the social deficits, an effect blocked by an oxytocin antagonist. We confirmed that oxytocin neurons mediated the behavioral improvement by activating endogenous oxytocin neurons in the paraventricular hypothalamus with Designer Receptors Exclusively Activated by Designer Drugs (DREADD). Last, we showed that chronic early postnatal treatment with oxytocin led to more lasting behavioral recovery and restored oxytocin immunoreactivity in the PVN. These data demonstrate dysregulation of the oxytocin system in *Cntnap2* knockout mice and suggest that there may be critical developmental windows for optimal treatment to rectify this deficit.

INTRODUCTION

Autism spectrum disorder (ASD) comprise a continuum of neurodevelopmental disorders characterized by core deficits in social behavior and communication, accompanied by restricted interests and repetitive behaviors (*1*). Other non-core symptoms frequently associated with ASD are epilepsy and hyperactivity, as well as sleep, sensory, and gastrointestinal abnormalities (*2*). Genetic studies have revealed extraordinary heterogeneity in ASD, predicting hundreds of rare risk genes, none accounting for more than 1% of ASD instances (*3–5*). These findings indicate that the study of rare, but highly penetrant, ASD susceptibility genes is likely to be of significant value. Further, among animal models for ASD, mouse models of monogenic forms of autism have the advantage of large effect size; several monogenic mouse models have high construct and face validity (*6*, *7*), but few have demonstrated potentially predictive validity for human therapeutics (*6*, *8*).

We have recently characterized a mouse knockout (KO) for the contactin-associated protein-like 2 (*Cntnap2*) gene, which is responsible for cortical dysplasia and focal epilepsy (CDFE) syndrome, a recessively inherited disorder in which 70% of affected individuals have ASD (*9*). Risperidone, an atypical antipsychotic used to treat irritability and other non-core behaviors in ASD, reduces hyperactivity, motor stereotypies, and perseveration in *Cntnap2* KO mice, but has no effect on the core autism behavior of sociability (*10*); these effects are similar to those observed in human patients. This differential efficacy supports the notion that distinct pathways lead to the social and repetitive behavioral deficits in ASD and suggests that this mouse model would be useful for testing new pharmacological treatments. For monogenic and polygenic ASD, no treatment consistently improves social behavior; currently approved pharmacotherapies target repetitive behavior and other non-core phenotypes.

The neuropeptide oxytocin (OXT) is involved in the modulation of various aspects of social behavior (*11*, *12*). A potential role for OXT in ASD is supported by genetic evidence from multiple investigations (*13–19*), although the power of these studies is limited by small sample sizes. A recent meta-analysis on variation in the OXT receptor with ASD found significant association with four single-nucleotide polymorphisms (*20*), but these findings were not genome-wide significant.

OXT is synthesized in two main regions of the hypothalamus, the supraoptic (SON) and paraventricular (PVN) nuclei. OXT-expressing neurons in the SON project mainly to the posterior pituitary and are responsible for OXT release into the peripheral bloodstream (*21*), where OXT has well-established neuroendocrine functions (*22*). OXT-expressing neurons in the PVN project to several brain regions, including the amygdala, hippocampus, and frontal cortex (*23*), where their role in behaviors such as fear, memory, and social behavior has recently been explored (*24*, *25*). Here, we performed limited in vivo screening for drugs that target social behavior in the *Cntnap2* mouse model.

[1]Program in Neurogenetics, Department of Neurology, David Geffen School of Medicine, University of California, Los Angeles, Los Angeles, CA 90095, USA. [2]Center for Autism Research and Treatment and Center for Neurobehavioral Genetics, Jane and Terry Semel Institute for Neuroscience and Human Behavior, University of California, Los Angeles, Los Angeles, CA 90095, USA. [3]Center for Neurobehavioral Genetics, Department of Psychiatry and Biobehavioral Sciences, University of California, Los Angeles, Los Angeles, CA 90095, USA. [4]Department of Molecular Cell Biology, Weizmann Institute of Science, Rehovot 76100, Israel. [5]Department of Psychiatry and Biobehavioral Sciences, Jane and Terry Semel Institute for Neuroscience and Human Behavior, University of California, Los Angeles, Los Angeles, CA 90095, USA. [6]Integrative Center for Learning and Memory, University of California, Los Angeles, Los Angeles, CA 90095, USA. [7]West Los Angeles VA Medical Center, Los Angeles, CA 90073, USA.
*Corresponding author. E-mail: dhg@ucla.edu

RESULTS

Oxytocin treatment rescues social behavior in *Cntnap2* KO mice

To search for a drug that could improve social behavior in ASD, we performed a limited, acute in vivo drug screen using five compounds that target molecular mechanisms putatively related to social behavior in *Cntnap2* KO mice and wild-type littermates using average doses selected from the literature (table S1). Groups consisted of juvenile (4 to 6 weeks old) mice, half male and half female. Preliminary analysis did not detect any sexual dimorphism in the response to treatment, so both sexes were analyzed as a single group, and equal numbers of males and females were used in all subsequent testing. Individual raw data for each experiment are shown in tables S2 to S21. Drugs were administered by intraperitoneal injection as an acute single dose, and mice were tested 20 to 30 min after administration with the reciprocal social interaction test. In this test, the time spent in social interaction by a pair of unfamiliar mice, matched for genotype, sex, age, and treatment, is measured (26). The reported time represents the combination of the behavior of the two animals within a pair. Analysis of the effect of treatment and genotype on social behavior by two-way analysis of variance (ANOVA) revealed a significant main effect of treatment ($F_{5,60} = 4.13$, $P = 0.0027$) and a genotype-treatment interaction that was not significant ($F_{5,60} = 2.23$, $P = 0.0627$). Pairwise comparisons to the vehicle-treated control (Dunnett's test) within genotypes revealed that *Cntnap2* mutant, but not wild-type mice, treated with the neuropeptides OXT and arginine vasopressin (AVP), showed improvements in juvenile social interaction ($P = 0.03$ and $P = 0.04$, respectively) (Fig. 1A). We confirmed this change in social behavior in an independent experiment with the widely used social approach (three-chamber) test performed in young adult mice at 6 to 8 weeks of age (Fig. 1B). In this test, mice are given the choice to interact with either an empty cup or a similar cup containing an unfamiliar stimulus mouse, matched for age and sex. The amount of time interacting with each cup is compared as a measurement of sociability, where normal sociability is defined as spending significantly more time interacting with
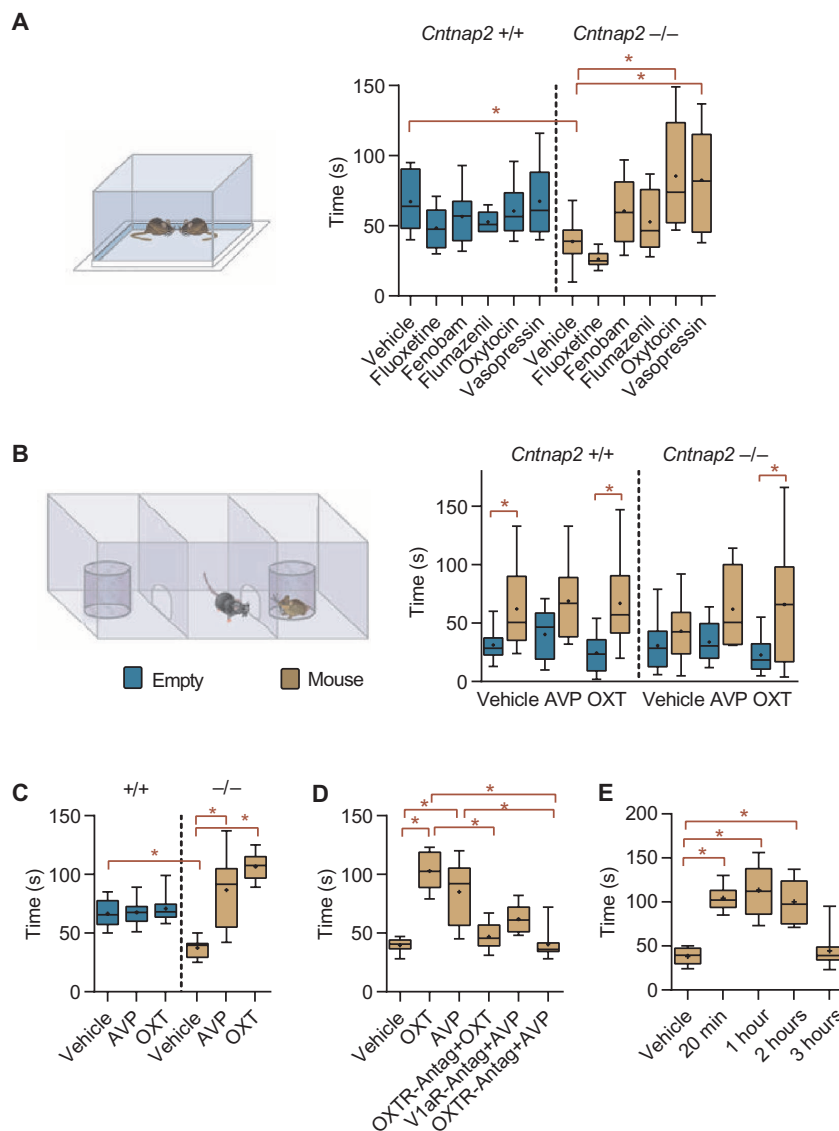

Fig. 1. Oxytocin administration rescues social behavior in the *Cntnap2* mouse model. (A) Reciprocal social interaction test for wild-type (WT) (left) and KO (right) drug- or vehicle-treated mice by intraperitoneal injection. The time spent engaged in social interaction for each pair of mice is shown ($n = 6$ pairs, 3M-3F, per genotype per condition). Two-way ANOVA $F_{11,60} = 2.89$, $P = 0.004$; treatment effect $F_{5,60} = 4.13$, $P = 0.0027$; treatment/genotype interaction $F_{5,60} = 2.23$, $P = 0.0627$, followed by Dunnett's pairwise comparisons to controls WT$_{vehicle}$-KO$_{vehicle}$ $P = 0.03$, KO$_{vehicle}$-KO$_{OXT}$ $P = 0.03$, KO$_{vehicle}$-KO$_{AVP}$ $P = 0.04$. **(B)** Social approach (three-chamber) test. Time spent interacting with an empty cup or a cup with a stranger mouse inside is shown for each genotype when treated intraperitoneally with vehicle, OXT, or AVP ($n = 8$ to 10, 4/5M-4/5F, mice per genotype per condition). Paired Student's t test comparing "mouse" to "empty" as a measure of sociability within each group. WT$_{vehicle}$ $P = 0.01$, WT$_{OXT}$ $P = 0.02$, KO$_{OXT}$ $P = 0.03$. **(C)** Reciprocal social interaction test when OXT and AVP are administered intranasally ($n = 8$, 4M-4F, pairs per genotype per condition). Two-way ANOVA $F_{5,42} = 15.88$, $P < 0.0001$; treatment effect $F_{2,42} = 21.08$, $P < 0.0001$; genotype/treatment interaction $F_{2,42} = 17.01$, $P \leq 0.0001$, followed by Dunnett's pairwise comparisons to controls WT$_{vehicle}$-KO$_{vehicle}$ $P < 0.0001$, KO$_{vehicle}$-KO$_{OXT}$ $P < 0.0001$, KO$_{vehicle}$-KO$_{AVP}$ $P < 0.0001$. **(D)** Reciprocal social interaction test ($n = 8$ pairs of mice, 4M-4F, per genotype per condition). One-way ANOVA $F_{5,41} = 22.02$, $P < 0.0001$, followed by Bonferroni post hoc test, modified significance level $P = 0.003$, all significant comparisons $P < 0.0001$. **(E)** Reciprocal social interaction test showing time course of a single acute dose of intranasal OXT administration ($n = 8$ pairs of mice, 4M-4F, per genotype per condition). One-way ANOVA $F_{4,35} = 23.16$, $P < 0.0001$, followed by Bonferroni post hoc test, modified significance level $P = 0.005$, all significant comparisons $P < 0.0001$. M, male; F, female. Box-plots represent the median plus the 25th and 75th percentiles. Whiskers represent the minimum and maximum values. The mean is represented by a plus sign. Asterisks represent a statistically significant difference between indicated groups.

the cup containing the mouse than with the empty cup (27, 28). Vehicle-treated wild-type mice showed normal sociability ($P = 0.01$), preferring to spend time interacting with the cup containing the other mouse; this pattern was not changed upon OXT treatment ($P = 0.02$). *Cntnap2* mutant mice, which at baseline showed no significant preference to interact with the cup containing the mouse over the empty cup ($P = 0.13$) (indicating a lack of sociability), strongly preferred to interact with the cup containing the mouse when treated with OXT ($P = 0.03$), but not with AVP ($P = 0.06$).

Although neuropeptides may cross the blood-brain barrier and reach the central nervous system, intranasal administration is a preferred way to target peptides to the brain without a need for invasive procedures (29). We therefore conducted an independent experiment in which we administered OXT or AVP intranasally and tested *Cntnap2* mutant mice for improvements in social behavior with the juvenile reciprocal social interaction test. Similar to what we found when the peptides were administered intraperitoneally, two-way ANOVA revealed a significant effect of treatment ($F_{2,42} = 21.08$, $P < 0.0001$) and a treatment-genotype interaction ($F_{2,42} = 17.01$, $P < 0.0001$). Pairwise comparisons to the control within genotypes showed that when administered intranasally, these neuropeptides have a similar or slightly larger effect (Dunnett's test; $P < 0.0001$ in both cases) on social behavior than when they are administered intraperitoneally to the *Cntnap2* mutant mice (Fig. 1C).

OXT and AVP are closely related nonapeptides that share high sequence and structure homology, differing only at residues 3 and 8. Although only one receptor exists for OXT in mammals, there are three different receptors for AVP: V1a, V1b, and V2, the V1a receptor being the predominant form in brain (11). AVP can bind and activate the OXT receptor. To better characterize the pathway implicated in the improvement in social behavior by both peptides, we blocked the peptide receptors before administering the drugs. We treated *Cntnap2* mutant juvenile animals (4 to 6 weeks old) with either an OXT receptor antagonist (L371,257) or an AVP-V1a receptor antagonist (relcovaptan), followed by either OXT or AVP, and performed behavioral tests 20 min after the agonist dose (Fig. 1D). One-way ANOVA revealed a significant effect of treatment on social behavior ($F_{5,41} = 22.02$, $P < 0.0001$). Post hoc analysis with Bonferroni correction for multiple comparisons showed that the behavioral improvement seen with OXT was abolished when the OXT receptor was blocked ($P < 0.0001$). In contrast, the behavioral effect of AVP was not abolished after AVP-V1a receptor block, but was eliminated by OXT receptor block ($P < 0.0001$). Although we cannot eliminate a minor contribution of the AVP system, these data suggest that the observed effect is mainly due to activation of the OXT receptor.

We performed additional behavioral tests to determine whether the improved social behavior seen in these animals upon OXT treatment was accompanied by other behavioral improvements. None of the other previously reported behavioral deficits, including hyperactivity, increased repetitive behavior, increased perseveration, and hypersensitivity to sensory stimuli, were rescued by administration of OXT (fig. S1). These data indicate that the behavioral effect of OXT administration seems restricted to the social behavior domain.

One potential limitation of OXT as a treatment for disorders of social cognition is its short half-life, proposed to be about 20 min in mammalian brain (30). Therefore, we assessed the time course of the OXT effect on social behavior with the reciprocal social interaction test, observing that the behavioral effect of a single intranasal treatment lasted for about 2 hours ($P < 0.0001$) in *Cntnap2* mice (Fig. 1E, one-way ANOVA of the time effect on treatment response, $F_{4,35} = 23.16$, $P < 0.0001$, followed by Bonferroni post hoc test). This result is in

accordance with a recent microdialysis study in which a single intranasal administration of OXT resulted in elevated brain OXT concentrations that lasted for about 90 min (31). It is also similar to behavioral effects on newborn macaques, in which OXT was correlated with increased social behavior 2 hours, but not 4 hours, after administration (32), and in neurotypical human volunteers and clinical studies (33), where behavioral testing was performed about 60 min after administration.

To extend our pharmacological results and explore the role of the endogenous OXT system, we took advantage of an emerging literature demonstrating that OXT neurons express a variety of receptors that can be pharmacologically targeted to stimulate endogenous OXT release, specifically the melanocortin and serotonin receptors. The melanocortin 4 receptor (MC4R) colocalizes with OXT neurons in the PVN (34). Stimulation of these receptors activates PVN OXT neurons in mice (35), induces central, but not peripheral, OXT release in rats (36), and promotes partner preference in voles (37). We treated wild-type and mutant mice with a selective MC4R agonist, Ro27-3225 (38), and tested its effect in a reciprocal social interaction test 30 min after treatment. Two-way ANOVA detected a genotype-treatment interaction ($F_{1,20} = 4.87$, $P = 0.04$), and pairwise comparisons to the vehicle-treated control (Dunnett's test) within genotypes showed that Ro27-3225 led to improvement ($P = 0.02$) in social behavior in the *Cntnap2* mouse (Fig. 2A). The behavioral effect of this drug was eliminated when the OXT receptor was blocked 15 min before administration (Fig. 2B, one-way ANOVA, $F_{2,18} = 14.60$, $P < 0.0001$, followed by Bonferroni post hoc test $P < 0.0001$), indicating that the effect is mediated through OXT release.

Cntnap2 KO mice show reduced number of OXT-expressing neurons

The improvement in social behavior upon OXT treatment was restricted to *Cntnap2* mutant mice and was not observed in wild-type
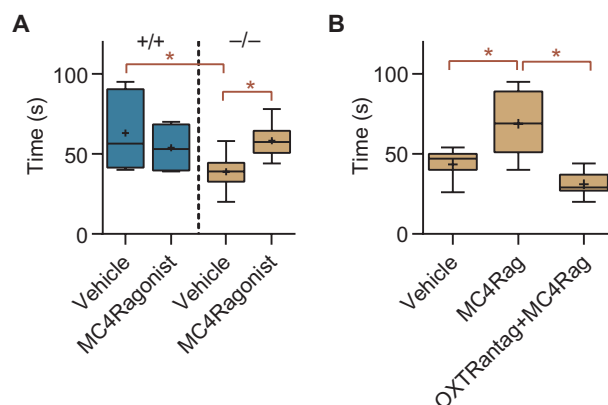

Fig. 2. Pharmacological stimulation of OXT release improves social behavior in the *Cntnap2* model. (A) Reciprocal social interaction test in vehicle- or drug-treated animals ($n = 6$ pairs of mice, 3M-3F, per genotype per condition). Two-way ANOVA genotype/treatment interaction $F_{1,20} = 4.87$, $P = 0.04$, followed by Dunnett's pairwise comparisons to controls, WT$_{vehicle}$-KO$_{vehicle}$ $P = 0.04$, KO$_{vehicle}$-KO$_{MC4Rag}$ $P = 0.02$. (B) Reciprocal social interaction test in *Cntnap2* KO ($n = 7$ pairs of mice, 4M-3F, per condition). One-way ANOVA $F_{2,18} = 14.6$, treatment effect $P \leq 0.0001$, followed by Bonferroni post hoc test, modified significance level $P = 0.017$, vehicle-agonist $P = 0.002$, agonist-antagonist $P < 0.0001$. M, male; F, female. Box-plots represent the median plus the 25th and 75th percentiles. Whiskers represent the minimum and maximum values. The mean is represented by a plus sign. Asterisks represent a statistically significant difference between indicated groups.

littermates (Fig. 1, A and C). This sensitivity to OXT in the mutant mice led us to hypothesize that the OXT system might itself be abnormal in *Cntnap2* KO mice. Expression of *Cntnap2* (*Caspr2*) has been conventionally associated with pyramidal excitatory neurons, a result of its well-established role in anchoring K⁺ channels at the nodes of Ranvier in myelinated axons (*39*). *Cntnap2* mRNA is also expressed in migrating GABAergic interneurons, where its function is still to be determined (*10*). In situ hybridization data from the Allen Mouse Brain Atlas ISH (in situ hybridization) database show that *Cntnap2* is strongly expressed in the hypothalamic PVN, where OXT neurons are clustered; we found by immunohistochemistry (IHC) that it is coexpressed in a subset of OXT-expressing neurons (fig. S2) in this region, suggesting a potential role for *Cntnap2* in the development or function of these diencephalic neurons.

To characterize the oxytocinergic system, we analyzed the number of OXT-expressing cells in the PVN of the hypothalamus at postnatal day 30 (P30), when the system is fully developed, and found that *Cntnap2* mutant mice have reduced numbers of OXT immunoreactive neurons compared to wild-type littermates (Fig. 3, A and B) (Student's *t* test, *P* = 0.03). To confirm this deficit, we measured OXT levels in whole-brain extracts by radioimmunoassay (RIA) and also found a significant reduction in OXT levels (Fig. 3C, Student's *t* test, *P* = 0.01). To determine whether this reduction was a result of fewer neurons (via death or development) or a lack of expression of the peptide within neurons, we counted the total number of neurons in the PVN and found no differences in the total number of neurons or in the total PVN area analyzed (fig. S3, A and B), indicating that it is OXT expression within neurons and not the number of neurons that is reduced. Because OXT and AVP neurons constitute most of PVN neurons, we also analyzed the number of AVP-expressing cells and found no difference between KO and wild-type mice (fig. S4).

Early postnatal subchronic administration of OXT has long-lasting behavioral effects

OXT is first detected by IHC during early postnatal life in rodents, gradually increasing in abundance from P7 until about weaning age (P21), when the system is considered fully developed (*40*, *41*). Consistent with this trajectory, we found many fewer OXT immunoreactive cells at P7 than at P30, and no differences between wild-type and KO mice at P7 (Fig. 4, A and B). The postnatal development of the OXT system suggests that OXT production may be especially vulnerable to early life manipulations. Both environmental (*42*, *43*) and pharmacological (*41*, *44*, *45*) manipulations during early postnatal life affect the central OXT system, as well as social behaviors, during adult life. In the prairie vole, a species widely used to study affiliative behavior such as pair bonding, a single intraperitoneal administration of OXT on P1 increases OXT immunoreactivity in the PVN at P21 (*41*) and strengthens partner preference at P60 (*44*, *45*). To test whether early postnatal OXT treatment affects social behavior in *Cntnap2* mice, we treated wild-type and KO littermates with daily intranasal administration of either saline or OXT from P7 to P21 and tested them 9 days later, at P30, with a social approach (three-chamber) test. We found that, as expected, saline-treated *Cntnap2* KO mice showed a lack of normal social interest, displaying no preference for the cup containing a mouse over the empty cup. In contrast, mice receiving daily postnatal OXT administration showed normal social behavior more than 1 week after cessation of the treatment (paired Student's *t* test, *P* = 0.004). Also, as expected, the normal sociability in wild-type littermates was unchanged (Fig. 5A).
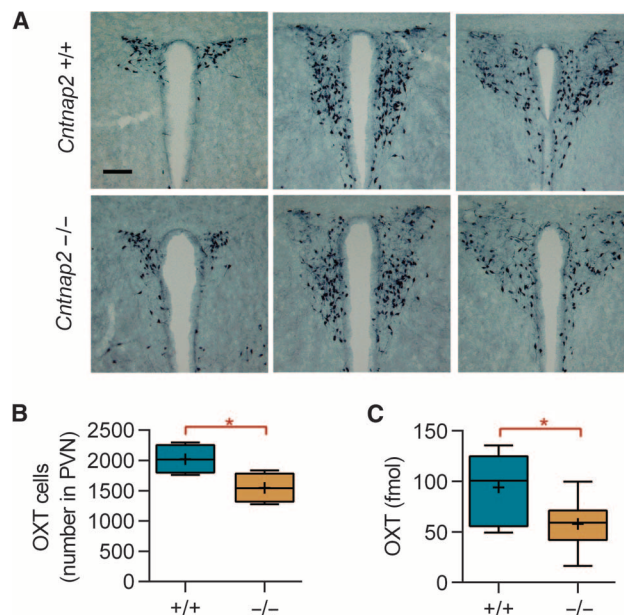

Fig. 3. *Cntnap2* mutant mice show reduced central OXT levels at P30. (**A**) Representative images of OXT immunoreactivity in different anteroposterior levels of the PVN in *Cntnap2* KO and WT controls at P30. Scale bar, 100 μm. (**B**) Stereological counts of OXT-positive cells in the PVN region of both genotypes at P30 (*n* = 4 mice, 2M-2F, per genotype). Student's *t* test, *P* = 0.03. (**C**) Quantification of OXT levels in whole-brain extracts by RIA at P30 (*n* = 10 mice, 5M-5F, per genotype). Student's *t* test, *P* = 0.01. M, male; F, female. Box-plots represent the median plus the 25th and 75th percentiles. Whiskers represent the minimum and maximum values. The mean is represented by a plus sign. Asterisks represent a statistically significant difference between indicated groups.
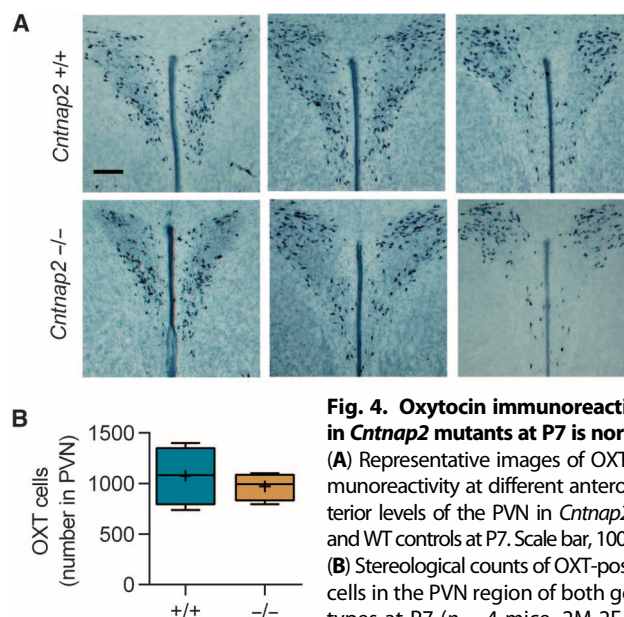

Fig. 4. Oxytocin immunoreactivity in *Cntnap2* mutants at P7 is normal. (**A**) Representative images of OXT immunoreactivity at different anteroposterior levels of the PVN in *Cntnap2* KO and WT controls at P7. Scale bar, 100 μm. (**B**) Stereological counts of OXT-positive cells in the PVN region of both genotypes at P7 (*n* = 4 mice, 2M-2F, per genotype). No differences were found with Student's *t* test (*P* = 0.53). M, male; F, female. Box-plots represent the median plus the 25th and 75th percentiles. Whiskers represent the minimum and maximum values. The mean is represented by a plus sign.

We confirmed the behavioral improvement in a second cohort of KO mice using the reciprocal social interaction test (Student's *t* test, *P* < 0.001), performed again at P30 (Fig. 5B). To test whether this improvement in social behavior correlated with an increase in endogenous OXT expression, we measured OXT levels in whole-brain extracts in these same animals and found that *Cntnap2* KO mice treated with OXT indeed showed a significant increase (Student's *t* test, *P* = 0.02) in endogenous OXT levels (Fig. 5C) relative to untreated KO mice. In addition, this increase in central OXT was correlated with an increased number of OXT immunoreactive neurons in the PVN of mutant mice (Student's *t* test, *P* = 0.005), which were rescued to nearly wild-type numbers by the postnatal OXT treatment regimen (Fig. 5, D and E). These data suggest that there may be an early developmental window during which treatment can achieve longer-lasting improvements in social behavior.

Stimulation of endogenous OXT neurons in the PVN rescues social behavior

To combine the pharmacological evidence for OXT modulation of social behavior with physiological data and directly test the hypothesis that PVN OXT neurons mediate the behavioral effects, we assessed whether activation of endogenous OXT release is sufficient for improving social behavior in *Cntnap2* mutant mice using DREADD (Designer Receptors Exclusively Activated by Designer Drugs) technology (*46*). We expressed a modified muscarinic acetylcholine receptor tagged with the fluorescent marker mCherry (hM3Dq-mCherry), which is exclusively activated by the otherwise inert ligand clozapine *N*-oxide (CNO), in OXT cells in the PVN by means of stereotaxic AAV2 injection. We restricted hM3Dq-mCherry expression to OXT cells by driving the expression with the OXT promoter (Fig. 6, A and B). Whole-cell, current-clamp recordings were performed in mCherry-expressing PVN neurons to confirm receptor efficiency in depolarizing OXT cells. When added to the bath, CNO (5 μM) depolarized and markedly increased the firing rate of OXT neurons (Fig. 6C). Next, we examined the behavioral effect of hM3Dq-mCherry activation in OXT cells. Thirty minutes after acute in vivo intraperitoneal administration of CNO (5 mg/kg), we observed normal social interest in the social approach (three-chamber) test in *Cntnap2* mice (paired Student's *t* test, *P* = 0.001), whereas vehicle-treated animals showed no preference for the cup containing the mouse. No CNO effect was seen on the normal sociability of wild-type animals (Fig. 6D), consistent with our previous findings using exogenous OXT administration.

DISCUSSION

Effective pharmacological treatments for social deficits in ASD are needed. The OXT system is a key mediator of social behavior in mammals, including humans, in many contexts such as maternal behavior, mother-infant bonding, social memory/recognition, and pair bonding (*12*, *47*). Mice with a genetically altered OXT system—such as KO mice for the OXT gene, the OXT receptor gene, or CD38 (a gene involved in OXT release)—all show social deficits that are restored upon OXT administration (*37*), and OXT is required for the rewarding properties of social stimuli in mice (*48*). In addition, OXT administration improves sociability in inbred mouse strains with naturally occurring lower sociability such as BALB/cByJ and C58/J (*49*). Thus, there is growing exploration of OXT's potential for therapeutic efficacy in ASD, with some studies showing a neurobiological evidence of mitiga-

tion of some aspects of social deficits in ASD (*50*, *51*). Given the etiological heterogeneity of ASD, a key issue is whether there are actual deficits in this system in some specific genetic forms of ASD because identifying which patients could potentially benefit the most from OXT treatment is critical (*52*). Studies addressing peripheral OXT levels in individuals with ASD have found both lower (*53*, *54*) and higher (*55*, *56*) values. Green *et al.* (*57*) reported lower levels of the peptide but higher levels of its precursor, suggesting a potential abnormality in its processing.
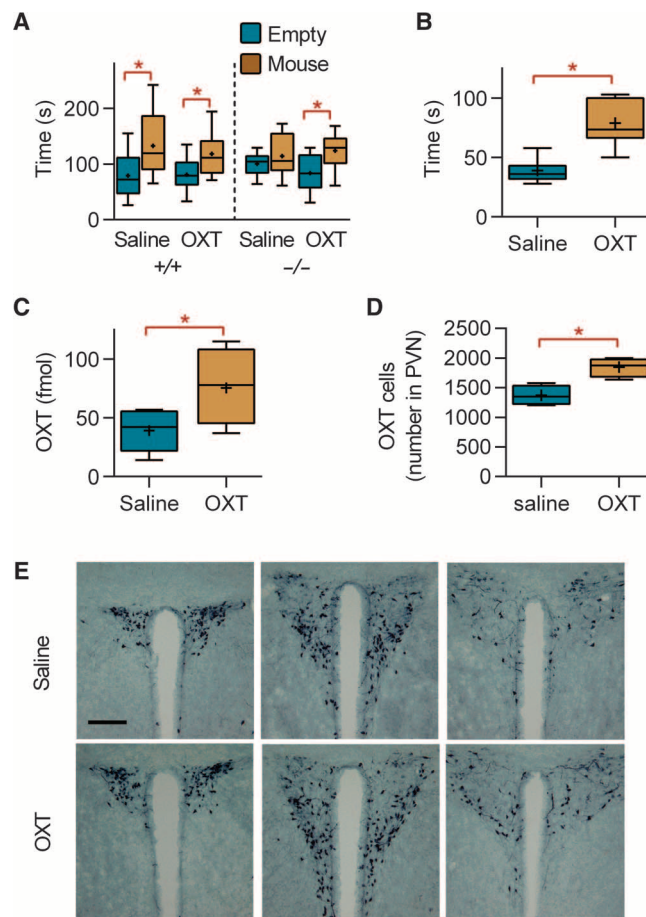

Fig. 5. Early postnatal OXT treatment restores peptide levels and improves social behavior at P30. (A) Social approach (three-chamber) test shown for WT and KO mice at P30 treated early with vehicle or OXT (*n* = 10 to 14 mice per group). Paired Student's *t* test comparing "mouse" to "empty" within each group as a measure of sociability, WT$_{saline}$ *P* = 0.006 (*n* = 10, 4M-6F), WT$_{OXT}$ *P* = 0.006 (*n* = 14, 8M-6F), KO$_{saline}$ *P* = 0.3 (*n* = 12, 6M-6F), KO$_{OXT}$ *P* = 0.004 (*n* = 13, 6M-7F). **(B)** Reciprocal social interaction test shown in pairs of KO mice at P30 treated early with saline or with OXT (*n* = 7 and 8 pairs of mice, 4M-3/4F, respectively). Student's *t* test, *P* < 0.001. **(C)** Quantification, as detected by RIA, of OXT levels in whole-brain extracts for KO mice treated with saline or OXT at P30 (*n* = 6, 3M-3F; *n* = 8, 4M-4F, respectively). Student's *t* test, *P* = 0.02. **(D)** Stereological quantification of the number of OXT immunoreactive cells in *Cntnap2* KO mice treated with either saline or OXT at P30 (*n* = 4 mice, 2M-2F, per condition). Student's *t* test, *P* = 0.005. **(E)** Representative images of OXT immunoreactivity in the PVN of saline- or OXT-treated KO animals at P30. Scale bar, 100 μm. M, male; F, female. Box-plots represent the median plus the 25th and 75th percentiles. Whiskers represent the minimum and maximum values. The mean is represented by a plus sign. Asterisks represent a statistically significant difference between indicated groups.
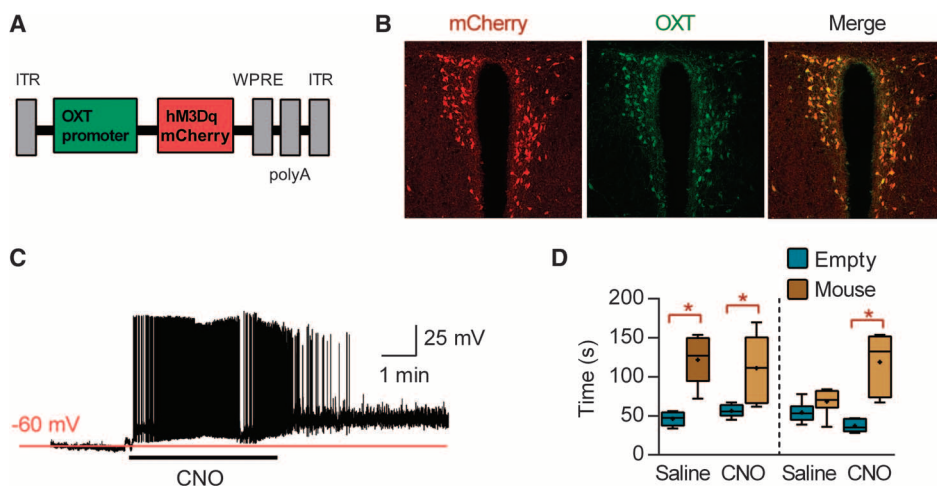
Fig. 6. Evoked OXT release improves social behavior in the *Cntnap2* mouse. (**A**) Schematic representation of the construct used to express designer receptors in OXT cells. WPRE, woodchuck hepatitis virus post-transcriptional regulatory element; ITR, inverted terminal repeat. (**B**) mCherry fluorescence in the PVN of AAV2-injected mice colocalizes with OXT immunoreactivity. (**C**) Representative trace of whole-cell, current-clamp recordings from an mCherry-labeled OXT neuron. CNO (5 μM) was perfused in the bath for 250 s, which resulted in consistent depolarization of membrane potential and an increase in action potential firing. (**D**) Social approach (three-chamber) test in saline- or CNO-treated (5 mg/kg) KO and WT mice (n = 6 male mice per genotype per condition). Paired Student's t test comparing "mouse" to "empty" within each group as a measure of sociability, WT_{saline} $P < 0.001$, WT_{CNO} $P = 0.03$, KO_{saline} $P = 0.13$, KO_{CNO} $P = 0.001$. Box-plots represent the median plus the 25th and 75th percentiles. Whiskers represent the minimum and maximum values. The mean is represented by a plus sign. Asterisks represent a statistically significant difference between indicated groups.

treatment in the KO mouse. This further suggested that drugs that induce endogenous OXT release would likely improve social behavior in this model. We observed that stimulation of MC4R, which activates PVN OXT neurons in mice (35) and induces central OXT release (36), also improved social behavior. There are a number of receptors on OXT neurons that could be targeted to induce OXT release (37). The further study of these receptors and the circuits in which they are implicated will help to develop therapeutic approaches based on manipulating this system.

Finally, we demonstrate that there may be an early developmental window that permits achievement of longer-lasting effects on symptoms, which suggests that early childhood treatment protocols could be relevant to some patients. Pharmacological manipulation of the OXT system during early postnatal life affects peptide levels and behavioral outcomes in adult rodents. Hammock and Levitt (59) have recently shown that neocortical OXT receptor binding in mice, similar to other rodents, shows a transient peak during early postnatal life, the period of major synaptic wiring and pruning, a result that could explain why this is a sensitive period for OXT in shaping neuronal circuits that ultimately mediate behavior. In prairie voles, a species widely used to study social behavior in the context of pair bonding, a single postnatal administration of OXT at P1 increases OXT in the hypothalamic PVN at weaning (41) and facilitates partner preference and alloparental care in young adulthood (44). Repeated OXT treatments during the first postnatal week increase the number of isolation-induced ultrasonic vocalizations (60), a measure of social vocal communication. In addition, daily neonatal treatment during this first week of life with a selective MC4R agonist promotes adult partner preference (61). Similarly, in mice, a single postnatal administration of OXT at P1 facilitated alloparental care and social approach in adulthood, whereas administration of an OXT antagonist produced the opposite effect (62) and subchronic OXT treatment in juvenile rats had long-lasting effects on social behavior, which was accompanied by increased plasma OXT concentrations (63). Although some of these studies used only male subjects (44, 63), others using both sexes found sexual dimorphism in their results, where treatment affected only males (62), only females (41, 60), or both (61). We found that a daily dose of OXT between P7 and P21 yielded effects on social behavior and increased peptide levels in brain extracts when analyzed 9 days later at P30 in both sexes. We attribute our results to our study of a monogenic, major gene model of ASD. It remains to be determined whether this change is permanent and whether this plasticity is present beyond early childhood.

Neuropeptides such as OXT contribute to network activity by modulating the effect of classical excitatory and inhibitory neurotransmitters. OXT stimulates fast-spiking parvalbumin interneuron activity, modulating circuit signal-to-noise ratio and improving information processing (64). Parvalbumin interneurons regulate network activity (65),

This apparent lack of consistency is not surprising because dysfunction in the OXT system can happen at different points in its regulation. Both the hormone itself (its synthesis, processing, storage, and release) and its receptor could be affected in pathological states. Although dysfunction in the OXT system is potentially associated with some forms of ASD, OXT has not yet emerged as a biomarker for disorders involving social cognition. Parker *et al.* (58) have recently shown that both OXT plasma concentration and OXTR (OXT receptor) polymorphisms affect individual differences in social functioning both in ASD and normal populations.

Here, we show in a validated mouse model of a monogenic form of ASD a clear reduction in OXT expression in the PVN of the hypothalamus, which is correlated with reduced OXT levels in brain extracts. Further, we demonstrate through multiple pharmacologic means that acute OXT treatment can rescue the observed social deficits in this mouse model. The effect lasts about 2 hours, similar to results in a recent study of newborn macaques, in which OXT was correlated with increased social behavior 2 hours, but not 4 hours, after administration (32). A similar time course is observed in multiple tasks performed by neurotypical human volunteers and in clinical studies (33), where behavioral testing was performed 60 min, or more, after administration. The long-lasting behavioral effect of a single dose, despite the short half-life of the peptide, has been proposed to be a result of its well-characterized self-priming process, in which OXT stimulates its own release in a positive feedback loop, presumably through activation of its own receptor (30). We also used an alternate pharmacophysiological approach, DREADD, to confirm that activation of PVN OXT neurons is sufficient to rescue the behavioral deficit, confirming the role of PVN OXT neurons in mediating the observed changes in social behavior with

and their dysfunction has been implicated in ASD. We previously found that the *Cntnap2* mouse shows deficits in GABAergic interneurons (*10*), and OXT receptor null mice have fewer GABAergic synapses (*66*). It is therefore possible that OXT compensates for GABAergic deficits in this mouse model. Although GABA (γ-aminobutyric acid) is inhibitory in adult brain, it is excitatory during fetal and early postnatal periods, and OXT is involved in its perinatal excitatory to inhibitory shift by reducing intracellular chloride levels (*67*). This process is altered in the *Fmr1* KO mouse, a model for fragile X syndrome, which also shows a reduced number of GABAergic interneurons (*68, 69*); preliminary results in the *Fmr1* KO suggest reduced OXT immunoreactivity in the PVN (*70*). Recent studies have reported effects of intranasal OXT in patients with fragile X syndrome, describing an improvement in eye gaze frequency during a social task, which suggests that OXT could be a potential treatment for social anxiety in this syndrome (*71*).

Our work opens an avenue for investigation of the precise molecular mechanisms of the effects of *Cntnap2* deletion on OXT neuron development. One possibility is that CNTNAP2, as a cell adhesion molecule, affects OXT neuron function through its well-established role in neuron-glia interaction (*39*). CNTNAP2 is expressed in OXT neurons, whose development and function depend on dynamic neuron-glia interactions (*72*). Alternatively, CNTNAP2 could be involved in the structural development of OXT neurons: Anderson *et al.* (*73*) have recently shown that CNTNAP2 has a role in neurite outgrowth, which is important for the proper development of neuronal circuits. In addition to studying molecular mechanisms, our model allows exploration of potential critical periods for OXT-induced behavioral effects, as well as potential effects on the seizure phenotype via GABA modulation (*65*).

A limitation of our study is that it does not determine which aspects of social behavior are affected by OXT. The standard behavioral tests do not distinguish among various forms of social approach or interaction. Further refinement of social testing after OXT or other treatments will be informative, as will the development of more naturalistic social testing. In addition, our results show OXT deficits in a single, specific genetic form of ASD, and the generality of the result is not known. Studying OXT in other defined genetic forms of ASD will be of value. A key goal remains to discern which forms of ASD show a direct or indirect dysregulation of this system because we suspect that these patients are the most likely to benefit from treatment with OXT. Such data, as well as a better understanding of optimal treatment timing, will be useful in designing more informed clinical trials.

MATERIALS AND METHODS

Study design
The main goal of this study was to explore the potential of different drugs to restore abnormal social behavior in the *Cntnap2* mouse model of ASD, which was measured as the time spent in social interaction with two different tests commonly used to assess social behavior in mouse models of ASD. A sample size of at least six mice per group was used for all behavioral testing, three to four mice per group were used for neuronal counting, and six to eight mice per group were used for biochemical studies. Exact numbers for each experiment are included in the figure legends. All groups consisted of half males and half females and were always matched among compared groups. Data collection was performed as described in the literature, and no exclusion criteria were applied. All analyses were performed blinded to genotype and/or

treatment. For drug treatments, animals were randomly assigned to treatment. No outliers were taken into account, and all collected data were used in statistical analyses.

Mice
Mutant mice lacking the *Cntnap2* gene (*Caspr2* null mice) were obtained from E. Peles (*39*) and backcrossed to the C57BL/6J background for over 12 generations. Experimental *Cntnap2* mutant and wild-type mice were obtained from heterozygous crossings. The day of birth was designated as P0. The three obtained genotypes were housed together, with three to four same-sex mice per cage. They were kept in 12-hour light/12-hour dark cycle and had ad libitum access to food and water. All procedures involving animals were performed in accordance with the University of California, Los Angeles (UCLA) and the Weizmann Institute of Science animal research committee, and the National Institutes of Health (NIH) *Guide for the Care and Use of Laboratory Animals*.

Immunohistochemistry
Mice were deeply anesthetized with Pentasol (sodium pentobarbital, 40 mg/kg body weight) and perfused intracardially, first with phosphate-buffered saline (PBS) followed by 4% paraformaldehyde (PFA) in PBS. The brains were removed, postfixed overnight in the same fixative, and cryoprotected by immersion in 30% sucrose in PBS for 3 to 5 days. Brains were embedded in optimum cutting temperature (OCT) compound, sectioned at a thickness of 50 μm on a cryostat, and used for free-floating IHC using standard fluorescence or avidin-biotin complex (ABC) methods (Vector Labs). Incubations with primary antibodies were performed overnight at 4°C and with secondary antibodies for 90 min at room temperature. For primary antibodies, we used rabbit anti-OXT (1:2000, ImmunoStar) and rabbit anti-AVP (1:2000, ImmunoStar). Appropriate secondary antibodies were either from the Alexa Fluor series from Invitrogen for fluorescence or from the biotinylated antibodies from Vector Labs. Images were acquired with a Zeiss LSM 510 laser scanning confocal microscope (fluorescence) or an Olympus BX51 microscope (brightfield).

X-galactosidase staining
Brains were obtained from 4% PFA-perfused mice and were subsequently cryoprotected in 30% sucrose in PBS overnight. Tissues were embedded in OCT compound (Tissue-Tek) and frozen on dry ice. Coronal sections (14 μm thick) were prepared with a cryostat. Staining was done with X-galactosidase (1 mg/ml) (Sigma) in 20 mM tris (pH 7.3), 5 mM ferricyanide, 5 mM ferrocyanide, 0.01% sodium deoxycholate, 0.02% NP-40, and 2 mM $MgCl_2$ in PBS overnight at 37°C.

Stereological analyses
Stereological analyses in the PVN were conducted as described (*74*) with minor modifications. Briefly, the PVN region defined by OXT or AVP staining was outlined bilaterally on live computer image using a 5× objective. The Stereo Investigator V10.42.1 software (MicroBrightField Inc.) placed a systematic random sampling grid (70 × 70 μm) within the selected area, giving ∼10 counting frames per area. A total of six to seven serial sections with periodicity $n = 2$ from each brain were counted bilaterally with a 40× objective to achieve optimal optical sectioning. For Nissl-stained cells, a double-staining OXT/Nissl was performed, the PVN area delimited by OXT staining was outlined, and Nissl-positive cells were counted with a 25 × 25–μm counting frame and a 100× oil immersion objective. The final postprocessing thickness of the sections

was 11 μm on average, so the counting frame height was kept at 9 μm for all sections studied to keep a 1-μm guard zone. The optical fractionator was used to estimate the total number of cells in the region of interest. The coefficient of error (Gundersen, $m = 1$) was 0.1 or less for all samples. All counts were made by the same investigator, who was blinded to the genotype/treatment of the mice.

Radioimmunoassay

To measure whole-brain OXT, mice were anesthetized with isoflurane and decapitated. The brain tissue was homogenized at room temperature in 10 ml of 1 N acetic acid using a Kinematika POLYTRON for 30 s at level 5. Samples were centrifuged at $1000g$ for 60 min at 4°C, and 7 ml of the resulting homogenate was neutralized with 1.2 ml of 5 N NaOH, 1.4 ml of 1 M Na_2HPO_4, and 0.4 ml of H_2O, and centrifuged at $15,000g$ for 60 min at 4°C. Samples were stored at −80°C until measured. The OXT RIA from Phoenix Pharmaceuticals Inc. was used as follows: the solid phase of the RIA was prepared by adding 50 μl of protein A solution dissolved in $NaHCO_3$ (pH 9) into 96-well flat-bottomed microtiter plates (Thermo Fisher) and incubated overnight at 40°C. The protein A solution was dumped, and the plate washed three times with wash buffer [0.15 M K_2HPO_4, 0.2 mM $C_6H_8O_6$, 0.1% gelatin, 0.1% Tween (pH 7.4)]. After the washes, 25 μl of antibody was added to each well and incubated for 4 hours at room temperature, after which the antibody solution was dumped and the plate washed three times. The standard (0.25 to 12.5 fmol) and samples were loaded in the volume of 25 μl per well and incubated for 24 hours at 40°C, and 10 μl of 5000 cpm ^{125}I OXT was added to each well and incubated overnight at 40°C. The plate was washed three times, 100 μl of MicroScint-20 (PerkinElmer) was added to each well, and the plate was counted for 4 min with a microplate scintillation counter (Packard).

Recombinant adeno-associated virus construction

We used a vector expressing a modified muscarinic receptor fused to the fluorescent protein mCherry (Addgene) [pAAV-hSyn-DIO-hM3D (Gq)-mCherry, plasmid #44361]. To drive the expression of the transgene from the OXT promoter, we first carried out in vitro Cre recombination to flip and remove the loxP sites in this construct and later exchanged the human synapsin promoter for a mouse OXT promoter consisting of 1 kb directly upstream of exon 1 of the OXT gene, which is sufficient to induce cell type–specific expression in OXT cells (75). The final plasmid was sent to the University of Pennsylvania Vector Core for custom AAV (adeno-associated virus) production (serotype 2).

Stereotaxic injection

Stereotaxic injections of 500 nl of an rAAV (recombinant adeno-associated virus) titer of ~10^{10} vector genome/ml were performed bilaterally in the PVN of the hypothalamus according to the following coordinates from bregma based on the Allen Brain Atlas: anteroposterior, −0.70 mm; dorsoventral, −5.20 mm; lateral, ±0.30 mm. Injections were performed at a rate of 100 nl/min with a glass micropipette (50-μm tip diameter) using a Nanoliter 2000 microinjection system [World Precision Instruments (WPI)] attached to a Micro4 pump (WPI). Behavioral and electrophysiological studies were performed 3 weeks after injections. The detailed method of stereotaxic injections can be found in (76).

Electrophysiological experiments

In vitro slice recordings were performed 3 weeks after injection of the rAAV into the PVN. Briefly, mice were deeply anesthetized with iso-

fluorane and beheaded. The brain was removed and set for cutting at a thickness of 300 μm on a Leica VT1000 S vibratome, while bathed in an ice-cold sucrose-based dissection solution containing 222 mM sucrose, 11 mM D-glucose, 26 mM $NaHCO_3$, 1 mM NaH_2PO_4, 3 mM KCl, 7 mM $MgCl_2$, 0.5 mM $CaCl_2$, aerated with 95% O_2, 5% CO_2. Slices containing the PVN were then allowed to recover for 30 min at 37°C in artificial cerebrospinal fluid (aCSF) containing 124 mM NaCl, 2.5 mM KCl, 26 mM $NaHCO_3$, 1.25 mM NaH_2PO_4, 10 mM D-glucose, 4 mM sucrose, 2.5 mM $CaCl_2$, 2 mM $MgCl_2$, aerated with 95% O_2, 5% CO_2, and subsequently transferred to room temperature until time of recording. The recording rig was continually perfused with aCSF, maintained at 32° to 34°C. Whole-cell recordings of PVN neurons were made in current-clamp mode, using a MultiClamp (Molecular Devices) patch-clamp amplifier. mCherry-positive neurons were identified via fluorescence microscopy, under visual guidance of differential interference contrast (DIC) optics with an Olympus BX51 microscope. Patch pipettes of 3 to 5 megohms were used, and filled with internal solution containing 115 mM potassium gluconate, 20 mM KCl, 10 mM Hepes, 10 mM phosphocreatine, 4 mM ATP (adenosine 5′-triphosphate)–Mg, and 0.3 mM GTP (guanosine 5′-triphosphate). Access resistance was less than 25 ohms and fully compensated in current-clamp mode. For pharmacological stimulation, 5 μM CNO (Sigma) was included in the aCSF bath perfusion. Neuronal responses were acquired and visualized with WinEDR (Strathclyde Electrophysiology Software).

Behavioral tests

Behavioral tests were performed in the UCLA behavioral test core and analyzed with the TopScan (CleverSys Inc.) automated system or by two independent experimenters blinded to genotype and treatment.

Open field

Mice were placed inside a clear Plexiglas arena (27.5 cm × 27.5 cm) for 20 min, and their general activity (distance traveled and velocity) was recorded. Results were analyzed with TopScan software (Clever Sys Inc.).

Reciprocal social interaction

Mice were placed in a cage to which they had been previously habituated (for 10 min) with an unfamiliar mouse matched in age, genotype, and sex for 10 min. Both mice in the pair were treated either with the same drug or with vehicle. The time engaged in social interaction (nose-to-nose sniffing, nose-to-anus sniffing, and following or crawling on/under each other) for the pair (combining the behavior of both animals) was measured by two independent human observers (26).

Social approach (three-chamber) test

The social approach test was performed as described (26). In brief, after 10 min of habituation, a mouse was placed in the central chamber of a clear Plexiglas box divided into three interconnected chambers and was given the choice to interact with either an empty wire cup (located in one side chamber) or a similar wire cup with an unfamiliar mouse inside (located in the opposite chamber), which was matched in age and sex. Time interacting with each cup was measured by two independent observers.

Drug administration

All drugs administered, dose used, and method of administration are summarized in table S1. All drugs were obtained from Sigma-Aldrich, except the OXT (L371,257) and AVP (relcovaptan) receptor antagonists, which were obtained from Tocris Bioscience. Doses were selected as an

average found in the literature for these compounds. For the initial drug screening, as well as for the receptor blocking experiments, all drugs were dissolved in 10% dimethyl sulfoxide in PBS, so that they all had the same vehicle control. For subsequent experiments, drugs were dissolved in saline. For intraperitoneal administration, drugs were administered in a volume of 10 ml/kg mouse weight (250 μl for an average 25-g mouse). For intranasal administration, a drop of 2.5-μl solution was placed in one of the animal's nostrils with a P10 pipette. Once the animal had aspirated the drop into its nasal cavity, the process was repeated for the other nostril. Pups (P7 to P21) each received 2 × 1.25-μl drop.

T maze spontaneous alternation

Mice were placed on the base of a T maze and were given the choice to explore either the right or left arm of the maze for 10 consecutive trials. Entry into an arm was registered once mice stepped with all four paws into the arm. At that moment, the gate to that arm was closed, and the animal was allowed to explore the arm for 5 s.

Grooming

Mice were individually caged, and the time spent grooming during a 10-min period after a 10-min acclimation was measured.

Hot plate test

Mice were placed on a heated plate (52.5°C), and the latency to paw withdrawal (up to 15 s) was measured.

Statistical analyses

Results are graphically presented as a box and whiskers plot. The whiskers extend from the minimum to the maximum value, and the box extends from the 25th to the 75th percentile. The median (50th percentile) is shown by a line, and the mean by a plus sign. One- or two-way ANOVA followed by Bonferroni post hoc tests in the case of multiple pairwise comparisons or Dunnett's test in the case of planned comparisons to a control as well as paired and unpaired two-tail Student's t test was used as indicated in each figure legend. F values, P values, and modified significance values after Bonferroni correction are presented in the figure legends. Data presentation and statistical analysis were performed with GraphPad software.

SUPPLEMENTARY MATERIALS

www.sciencetranslationalmedicine.org/cgi/content/full/7/271/271ra8/DC1

Fig. S1. No OXT effect on non-core–associated behavioral deficits in the *Cntnap2* mouse model.
Fig. S2. *Cntnap2*/OXT colocalization in the PVN.
Fig. S3. Total number of neurons in the PVN area.
Fig. S4. Vasopressin immunoreactivity in the PVN.
Fig. S5. Map and sequence for the hM3Dq-mCherry construct.
Table S1. Drugs used for pharmacological testing.
Table S2. Raw data of Fig. 1A.
Table S3. Raw data of Fig. 1B.
Table S4. Raw data of Fig. 1C.
Table S5. Raw data of Fig. 1D.
Table S6. Raw data of Fig. 1E.
Table S7. Raw data of Fig. 2A.
Table S8. Raw data of Fig. 2B.
Table S9. Raw data of Fig. 3.
Table S10. Raw data of Fig. 4.
Table S11. Raw data of Fig. 5A.
Table S12. Raw data of Fig. 5B.
Table S13. Raw data of Fig. 5C.
Table S14. Raw data of Fig. 5D.
Table S15. Raw data of Fig. 6.
Table S16. Raw data of fig. S1A.
Table S17. Raw data of fig. S1B.
Table S18. Raw data of fig. S1C.
Table S19. Raw data of fig. S1D.
Table S20. Raw data of fig. S3.
Table S21. Raw data of fig. S4.

REFERENCES AND NOTES

1. American Psychiatric Association, *Diagnostic and Statistical Manual of Mental Disorders* (American Psychiatric Publishing, Washington, DC, ed. 5 2013).
2. D. H. Geschwind, Advances in autism. *Annu. Rev. Med.* **60**, 367–380 (2009).
3. I. Iossifov, B. J. O'Roak, S. J. Sanders, M. Ronemus, N. Krumm, D. Levy, H. A. Stessman, K. T. Witherspoon, L. Vives, K. E. Patterson, J. D. Smith, B. Paeper, D. A. Nickerson, J. Dea, S. Dong, L. E. Gonzalez, J. D. Mandell, S. M. Mane, M. T. Murtha, C. A. Sullivan, M. F. Walker, Z. Waqar, L. Wei, A. J. Willsey, B. Yamrom, Y. H. Lee, E. Grabowska, E. Dalkic, Z. Wang, S. Marks, P. Andrews, A. Leotta, J. Kendall, I. Hakker, J. Rosenbaum, B. Ma, L. Rodgers, J. Troge, G. Narzisi, S. Yoon, M. C. Schatz, K. Ye, W. R. McCombie, J. Shendure, E. E. Eichler, M. W. State, M. Wigler, The contribution of de novo coding mutations to autism spectrum disorder. *Nature* **515**, 216–221 (2014).
4. S. De Rubeis, X. He, A. P. Goldberg, C. S. Poultney, K. Samocha, A. E. Cicek, Y. Kou, L. Liu, M. Fromer, S. Walker, T. Singh, L. Klei, J. Kosmicki, F. Shih-Chen, B. Aleksic, M. Biscaldi, P. F. Bolton, J. M. Brownfeld, J. Cai, N. G. Campbell, A. Carracedo, M. H. Chahrour, A. G. Chiocchetti, H. Coon, E. L. Crawford, S. R. Curran, G. Dawson, E. Duketis, B. A. Fernandez, L. Gallagher, E. Geller, S. J. Guter, R. S. Hill, J. Ionita-Laza, P. Jimenz Gonzalez, H. Kilpinen, S. M. Klauck, A. Kolevzon, I. Lee, I. Lei, J. Lei, T. Lehtimäki, C. F. Lin, A. Ma'ayan, C. R. Marshall, A. L. McInnes, B. Neale, M. J. Owen, N. Ozaki, M. Parellada, J. R. Parr, S. Purcell, K. Puura, D. Rajagopalan, K. Rehnström, A. Reichenberg, A. Sabo, M. Sachse, S. J. Sanders, C. Schafer, M. Schulte-Rüther, D. Skuse, C. Stevens, P. Szatmari, K. Tammimies, O. Valladares, A. Voran, W. Li-San, L. A. Weiss, A. J. Willsey, T. W. Yu, K. Yuen; DDD Study; Homozygosity Mapping Collaborative for Autism; UK10K Consortium, E. H. Cook, C. M. Freitag, M. Gill, C. M. Hultman, T. Lehner, A. Palotie, G. D. Schellenberg, P. Sklar, M. W. State, J. S. Sutcliffe, C. A. Walsh, S. W. Scherer, M. E. Zwick, J. C. Barett, D. J. Cutler, K. Roeder, B. Devlin, M. J. Daly, J. D. Buxbaum, Synaptic, transcriptional and chromatin genes disrupted in autism. *Nature* **515**, 209–215 (2014).
5. J. M. Berg, D. H. Geschwind, Autism genetics: Searching for specificity and convergence. *Genome Biol.* **13**, 247 (2012).
6. H. Won, W. Mah, E. Kim, Autism spectrum disorder causes, mechanisms, and treatments: Focus on neuronal synapses. *Front. Mol. Neurosci.* **6**, 19 (2013).
7. E. Ey, C. S. Leblond, T. Bourgeron, Behavioral profiles of mouse models for autism spectrum disorders. *Autism Res.* **4**, 5–16 (2011).
8. J. N. Crawley, Translational animal models of autism and neurodevelopmental disorders. *Dialogues Clin. Neurosci.* **14**, 293–305 (2012).
9. K. A. Strauss, E. G. Puffenberger, M. J. Huentelman, S. Gottlieb, S. E. Dobrin, J. M. Parod, D. A. Stephan, D. H. Morton, Recessive symptomatic focal epilepsy and mutant contactin-associated protein-like 2. *N. Engl. J. Med.* **354**, 1370–1377 (2006).
10. O. Peñagarikano, B. S. Abrahams, E. I. Herman, K. D. Winden, A. Gdalyahu, H. Dong, L. I. Sonnenblick, R. Gruver, J. Almajano, A. Bragin, P. Golshani, J. T. Trachtenberg, E. Peles, D. H. Geschwind, Absence of CNTNAP2 leads to epilepsy, neuronal migration abnormalities, and core autism-related deficits. *Cell* **147**, 235–246 (2011).
11. T. R. Insel, The challenge of translation in social neuroscience: A review of oxytocin, vasopressin, and affiliative behavior. *Neuron* **65**, 768–779 (2010).
12. H. E. Ross, L. J. Young, Oxytocin and the neural mechanisms regulating social cognition and affiliative behavior. *Front. Neuroendocrinol.* **30**, 534–547 (2009).
13. S. Wu, M. Jia, Y. Ruan, J. Liu, Y. Guo, M. Shuang, X. Gong, Y. Zhang, X. Yang, D. Zhang, Positive association of the oxytocin receptor gene (*OXTR*) with autism in the Chinese Han population. *Biol. Psychiatry* **58**, 74–77 (2005).
14. R. P. Ebstein, S. Israel, E. Lerer, F. Uzefovsky, I. Shalev, I. Gritsenko, M. Riebold, S. Salomon, N. Yirmiya, Arginine vasopressin and oxytocin modulate human social behavior. *Ann. N.Y. Acad. Sci.* **1167**, 87–102 (2009).
15. E. Lerer, S. Levi, S. Salomon, A. Darvasi, N. Yirmiya, R. P. Ebstein, Association between the oxytocin receptor (*OXTR*) gene and autism: Relationship to Vineland Adaptive Behavior Scales and cognition. *Mol. Psychiatry* **13**, 980–988 (2008).
16. E. Lerer, S. Levi, S. Israel, M. Yaari, L. Nemanov, D. Mankuta, Y. Nurit, R. P. Ebstein, Low CD38 expression in lymphoblastoid cells and haplotypes are both associated with autism in a family-based study. *Autism Res.* **3**, 293–302 (2010).
17. T. Munesue, S. Yokoyama, K. Nakamura, A. Anitha, K. Yamada, K. Hayashi, T. Asaka, H. X. Liu, D. Jin, K. Koizumi, M. S. Islam, J. J. Huang, W. J. Ma, U. H. Kim, S. J. Kim, K. Park, D. Kim, M. Kikuchi, Y. Ono, H. Nakatani, S. Suda, T. Miyachi, H. Hirai, A. Salmina, Y. A. Pichugina, A. A. Soumarokov,

N. Takei, N. Mori, M. Tsujii, T. Sugiyama, K. Yagi, M. Yamagishi, T. Sasaki, H. Yamasue, N. Kato, R. Hashimoto, M. Taniike, Y. Hayashi, J. Hamada, S. Suzuki, A. Ooi, M. Noda, Y. Kamiyama, M. A. Kido, O. Lopatina, M. Hashii, S. Amina, F. Malavasi, E. J. Huang, J. Zhang, N. Shimizu, T. Yoshikawa, A. Matsushima, Y. Minabe, H. Higashida, Two genetic variants of CD38 in subjects with autism spectrum disorder and controls. *Neurosci. Res.* **67**, 181–191 (2010).

18. A. K. Wermter, I. Kamp-Becker, P. Hesse, G. Schulte-Körne, K. Strauch, H. Remschmidt, Evidence for the involvement of genetic variation in the *oxytocin receptor gene* (*OXTR*) in the etiology of autistic disorders on high-functioning level. *Am. J. Med. Genet. B Neuropsychiatr. Genet.* **153B**, 629–639 (2010).

19. D. H. Skuse, A. Lori, J. F. Cubells, I. Lee, K. N. Conneely, K. Puura, T. Lehtimäki, E. B. Binder, L. J. Young, Common polymorphism in the *oxytocin receptor gene* (*OXTR*) is associated with human social recognition skills. *Proc. Natl. Acad. Sci. U.S.A.* **111**, 1987–1992 (2014).

20. D. LoParo, I. D. Waldman, The oxytocin receptor gene (OXTR) is associated with autism spectrum disorder: A meta-analysis. *Mol. Psychiatry* 10.1038/mp.2014.77 (2014).

21. M. J. Brownstein, J. T. Russell, H. Gainer, Synthesis, transport, and release of posterior pituitary hormones. *Science* **207**, 373–378 (1980).

22. A. Kiss, J. D. Mikkelsen, Oxytocin—Anatomy and functional assignments: A minireview. *Endocr. Regul.* **39**, 97–105 (2005).

23. H. S. Knobloch, A. Charlet, L. C. Hoffmann, M. Eliava, S. Khrulev, A. H. Cetin, P. Osten, M. K. Schwarz, P. H. Seeburg, R. Stoop, V. Grinevich, Evoked axonal oxytocin release in the central amygdala attenuates fear response. *Neuron* **73**, 553–566 (2012).

24. R. Stoop, Neuromodulation by oxytocin and vasopressin. *Neuron* **76**, 142–159 (2012).

25. H. J. Lee, A. H. Macbeth, J. H. Pagani, W. S. Young III, Oxytocin: The great facilitator of life. *Prog. Neurobiol.* **88**, 127–151 (2009).

26. J. L. Silverman, M. Yang, C. Lord, J. N. Crawley, Behavioural phenotyping assays for mouse models of autism. *Nat. Rev. Neurosci.* **11**, 490–502 (2010).

27. J. L. Silverman, D. G. Smith, S. J. Rizzo, M. N. Karras, S. M. Turner, S. S. Tolu, D. K. Bryce, D. L. Smith, K. Fonseca, R. H. Ring, J. N. Crawley, Negative allosteric modulation of the mGluR5 receptor reduces repetitive behaviors and rescues social deficits in mouse models of autism. *Sci. Transl. Med.* **4**, 131ra51 (2012).

28. S. E. Smith, Y. D. Zhou, G. Zhang, Z. Jin, D. C. Stoppel, M. P. Anderson, Increased gene dosage of *Ube3a* results in autism traits and decreased glutamate synaptic transmission in mice. *Sci. Transl. Med.* **3**, 103ra97 (2011).

29. C. D. Chapman, W. H. Frey II, S. Craft, L. Danielyan, M. Hallschmid, H. B. Schiöth, C. Benedict, Intranasal treatment of central nervous system dysfunction in humans. *Pharm. Res.* **30**, 2475–2484 (2013).

30. M. Ludwig, G. Leng, Dendritic peptide release and peptide-dependent behaviours. *Nat. Rev. Neurosci.* **7**, 126–136 (2006).

31. I. D. Neumann, R. Maloumby, D. I. Beiderbeck, M. Lukas, R. Landgraf, Increased brain and plasma oxytocin after nasal and peripheral administration in rats and mice. *Psychoneuroendocrinology* **38**, 1985–1993 (2013).

32. E. A. Simpson, V. Sclafani, A. Paukner, A. F. Hamel, M. A. Novak, J. S. Meyer, S. J. Suomi, P. F. Ferrari, Inhaled oxytocin increases positive social behaviors in newborn macaques. *Proc. Natl. Acad. Sci. U.S.A.* **111**, 6922–6927 (2014).

33. N. Striepens, K. M. Kendrick, W. Maier, R. Hurlemann, Prosocial effects of oxytocin and clinical evidence for its therapeutic potential. *Front. Neuroendocrinol.* **32**, 426–450 (2011).

34. J. E. Siljee, U. A. Unmehopa, A. Kalsbeek, D. F. Swaab, E. Fliers, A. Alkemade, Melanocortin 4 receptor distribution in the human hypothalamus. *Eur. J. Endocrinol.* **168**, 361–369 (2013).

35. B. M. Kublaoui, T. Gemelli, K. P. Tolson, Y. Wang, A. R. Zinn, Oxytocin deficiency mediates hyperphagic obesity of *Sim1* haploinsufficient mice. *Mol. Endocrinol.* **22**, 1723–1734 (2008).

36. N. Sabatier, α-Melanocyte–stimulating hormone and oxytocin: A peptide signalling cascade in the hypothalamus. *J. Neuroendocrinol.* **18**, 703–710 (2006).

37. M. E. Modi, L. J. Young, The oxytocin system in drug discovery for autism: Animal models and novel therapeutic strategies. *Horm. Behav.* **61**, 340–350 (2012).

38. S. C. Benoit, M. W. Schwartz, J. L. Lachey, M. M. Hagan, P. A. Rushing, K. A. Blake, K. A. Yagaloff, G. Kurylko, L. Franco, W. Danhoo, R. J. Seeley, A novel selective melanocortin-4 receptor agonist reduces food intake in rats and mice without producing aversive consequences. *J. Neurosci.* **20**, 3442–3448 (2000).

39. S. Poliak, D. Salomon, H. Elhanany, H. Sabanay, B. Kiernan, L. Pevny, C. L. Stewart, X. Xu, S. Y. Chiu, P. Shrager, A. J. Furley, E. Peles, Juxtaparanodal clustering of *Shaker*-like K⁺ channels in myelinated axons depends on Caspr2 and TAG-1. *J. Cell Biol.* **162**, 1149–1160 (2003).

40. E. F. Lipari, D. Lipari, A. Gerbino, D. Di Liberto, M. Bellafiore, M. Catalano, B. Valentino, The hypothalamic magnocellular neurosecretory system in developing rats. *Eur. J. Histochem.* **45**, 163–168 (2001).

41. Y. Yamamoto, B. S. Cushing, K. M. Kramer, P. D. Epperson, G. E. Hoffman, C. S. Carter, Neonatal manipulations of oxytocin alter expression of oxytocin and vasopressin immunoreactive cells in the paraventricular nucleus of the hypothalamus in a gender-specific manner. *Neuroscience* **125**, 947–955 (2004).

42. J. J. Zheng, S. J. Li, X. D. Zhang, W. Y. Miao, D. Zhang, H. Yao, X. Yu, Oxytocin mediates early experience–dependent cross-modal plasticity in the sensory cortices. *Nat. Neurosci.* **17**, 391–399 (2014).

43. T. H. Ahern, L. J. Young, The impact of early life family structure on adult social attachment, alloparental behavior, and the neuropeptide systems regulating affiliative behaviors in the monogamous prairie vole (*Microtus ochrogaster*). *Front. Behav. Neurosci.* **3**, 17 (2009).

44. K. L. Bales, C. S. Carter, Developmental exposure to oxytocin facilitates partner preferences in male prairie voles (*Microtus ochrogaster*). *Behav. Neurosci.* **117**, 854–859 (2003).

45. H. E. Ross, C. D. Cole, Y. Smith, I. D. Neumann, R. Landgraf, A. Z. Murphy, L. J. Young, Characterization of the oxytocin system regulating affiliative behavior in female prairie voles. *Neuroscience* **162**, 892–903 (2009).

46. H. M. Lee, P. M. Giguere, B. L. Roth, DREADDs: Novel tools for drug discovery and development. *Drug Discov. Today* **19**, 469–473 (2014).

47. C. McCall, T. Singer, The animal and human neuroendocrinology of social cognition, motivation and behavior. *Nat. Neurosci.* **15**, 681–688 (2012).

48. G. Dölen, A. Darvishzadeh, K. W. Huang, R. C. Malenka, Social reward requires coordinated activity of nucleus accumbens oxytocin and serotonin. *Nature* **501**, 179–184 (2013).

49. B. L. Teng, R. J. Nonneman, K. L. Agster, V. D. Nikolova, T. T. Davis, N. V. Riddick, L. K. Baker, C. A. Pedersen, M. B. Jarstfer, S. S. Moy, Prosocial effects of oxytocin in two mouse models of autism spectrum disorders. *Neuropharmacology* **72**, 187–196 (2013).

50. Y. Aoki, N. Yahata, T. Watanabe, Y. Takano, Y. Kawakubo, H. Kuwabara, N. Iwashiro, T. Natsubori, H. Inoue, M. Suga, H. Takao, H. Sasaki, W. Gonoi, A. Kunimatsu, K. Kasai, H. Yamasue, Oxytocin improves behavioural and neural deficits in inferring others' social emotions in autism. *Brain* **137**, 3073–3086 (2014).

51. T. Watanabe, O. Abe, H. Kuwabara, N. Yahata, Y. Takano, N. Iwashiro, T. Natsubori, Y. Aoki, H. Takao, Y. Kawakubo, Y. Kamio, N. Kato, Y. Miyashita, K. Kasai, H. Yamasue, Mitigation of sociocommunicational deficits of autism through oxytocin-induced recovery of medial prefrontal activity: A randomized trial. *JAMA Psychiatry* **71**, 166–175 (2014).

52. D. M. Cochran, D. Fallon, M. Hill, J. A. Frazier, The role of oxytocin in psychiatric disorders: A review of biological and therapeutic research findings. *Harv. Rev. Psychiatry* **21**, 219–247 (2013).

53. C. Modahl, L. Green, D. Fein, M. Morris, L. Waterhouse, C. Feinstein, H. Levin, Plasma oxytocin levels in autistic children. *Biol. Psychiatry* **43**, 270–277 (1998).

54. E. Andari, J. R. Duhamel, T. Zalla, E. Herbrecht, M. Leboyer, A. Sirigu, Promoting social behavior with oxytocin in high-functioning autism spectrum disorders. *Proc. Natl. Acad. Sci. U.S.A.* **107**, 4389–4394 (2010).

55. L. M. Jansen, C. C. Gispen-de Wied, V. M. Wiegant, H. G. Westenberg, B. E. Lahuis, H. van Engeland, Autonomic and neuroendocrine responses to a psychosocial stressor in adults with autistic spectrum disorder. *J. Autism Dev. Disord.* **36**, 891–899 (2006).

56. J. D. Jacobson, K. A. Ellerbeck, K. A. Kelly, K. K. Fleming, T. R. Jamison, C. W. Coffey, C. M. Smith, R. M. Reese, S. A. Sands, Evidence for alterations in stimulatory G proteins and oxytocin levels in children with autism. *Psychoneuroendocrinology* **40**, 159–169 (2014).

57. L. Green, D. Fein, C. Modahl, C. Feinstein, L. Waterhouse, M. Morris, Oxytocin and autistic disorder: Alterations in peptide forms. *Biol. Psychiatry* **50**, 609–613 (2001).

58. K. J. Parker, J. P. Garner, R. A. Libove, S. A. Hyde, K. B. Hornbeak, D. S. Carson, C. P. Liao, J. M. Phillips, J. F. Hallmayer, A. Y. Hardan, Plasma oxytocin concentrations and *OXTR* polymorphisms predict social impairments in children with and without autism spectrum disorder. *Proc. Natl. Acad. Sci. U.S.A.* **111**, 12258–12263 (2014).

59. E. A. Hammock, P. Levitt, Oxytocin receptor ligand binding in embryonic tissue and postnatal brain development of the C57BL/6J mouse. *Front. Behav. Neurosci.* **7**, 195 (2013).

60. K. M. Kramer, C. Choe, C. S. Carter, B. S. Cushing, Developmental effects of oxytocin on neural activation and neuropeptide release in response to social stimuli. *Horm. Behav.* **49**, 206–214 (2006).

61. C. E. Barrett, M. E. Modi, B. C. Zhang, H. Walum, K. Inoue, L. J. Young, Neonatal melanocortin receptor agonist treatment reduces play fighting and promotes adult attachment in prairie voles in a sex-dependent manner. *Neuropharmacology* **85**, 357–366 (2014).

62. K. Mogi, R. Ooyama, M. Nagasawa, T. Kikusui, Effects of neonatal oxytocin manipulation on development of social behaviors in mice. *Physiol. Behav.* **133**, 68–75 (2014).

63. A. S. Suraev, M. T. Bowen, S. O. Ali, C. Hicks, L. Ramos, I. S. McGregor, Adolescent exposure to oxytocin, but not the selective oxytocin receptor agonist TGOT, increases social behavior and plasma oxytocin in adulthood. *Horm. Behav.* **65**, 488–496 (2014).

64. S. F. Owen, S. N. Tuncdemir, P. L. Bader, N. N. Tirko, G. Fishell, R. W. Tsien, Oxytocin enhances hippocampal spike transmission by modulating fast-spiking interneurons. *Nature* **500**, 458–462 (2013).

65. V. S. Sohal, F. Zhang, O. Yizhar, K. Deisseroth, Parvalbumin neurons and gamma rhythms enhance cortical circuit performance. *Nature* **459**, 698–702 (2009).

66. M. Sala, D. Braida, D. Lentini, M. Busnelli, E. Bulgheroni, V. Capurro, A. Finardi, A. Donzelli, L. Pattini, T. Rubino, D. Parolaro, K. Nishimori, M. Parenti, B. Chini, Pharmacologic rescue of impaired cognitive flexibility, social deficits, increased aggression, and seizure susceptibility in oxytocin receptor null mice: A neurobehavioral model of autism. *Biol. Psychiatry* **69**, 875–882 (2011).

67. R. Tyzio, R. Cossart, I. Khalilov, M. Minlebaev, C. A. Hübner, A. Represa, Y. Ben-Ari, R. Khazipov, Maternal oxytocin triggers a transient inhibitory switch in GABA signaling in the fetal brain during delivery. *Science* **314**, 1788–1792 (2006).

68. R. Tyzio, R. Nardou, D. C. Ferrari, T. Tsintsadze, A. Shahrokhi, S. Eftekhari, I. Khalilov, V. Tsintsadze, C. Brouchoud, G. Chazal, E. Lemonnier, N. Lozovaya, N. Burnashev, Y. Ben-Ari, Oxytocin-mediated GABA inhibition during delivery attenuates autism pathogenesis in rodent offspring. *Science* **343**, 675–679 (2014).

69. L. Selby, C. Zhang, Q. Q. Sun, Major defects in neocortical GABAergic inhibitory circuits in mice lacking the fragile X mental retardation protein. *Neurosci. Lett.* **412**, 227–232 (2007).

70. S. M. Francis, A. Sagar, T. Levin-Decanini, W. Liu, C. S. Carter, S. Jacob, Oxytocin and vasopressin systems in genetic syndromes and neurodevelopmental disorders. *Brain Res.* **1580**, 199–218 (2014).

71. S. S. Hall, A. A. Lightbody, B. E. McCarthy, K. J. Parker, A. L. Reiss, Effects of intranasal oxytocin on social anxiety in males with fragile X syndrome. *Psychoneuroendocrinology* **37**, 509–518 (2012).

72. D. T. Theodosis, M. Schachner, I. D. Neumann, Oxytocin neuron activation in NCAM-deficient mice: Anatomical and functional consequences. *Eur. J. Neurosci.* **20**, 3270–3280 (2004).

73. G. R. Anderson, T. Galfin, W. Xu, J. Aoto, R. C. Malenka, T. C. Südhof, Candidate autism gene screen identifies critical role for cell-adhesion molecule CASPR2 in dendritic arborization and spine development. *Proc. Natl. Acad. Sci. U.S.A.* **109**, 18120–18125 (2012).

74. K. P. Tolson, T. Gemelli, L. Gautron, J. K. Elmquist, A. R. Zinn, B. M. Kublaoui, Postnatal *Sim1* deficiency causes hyperphagic obesity and reduced *Mc4r* and *oxytocin* expression. *J. Neurosci.* **30**, 3803–3812 (2010).

75. R. L. Fields, T. A. Ponzio, M. Kawasaki, H. Gainer, Cell-type specific oxytocin gene expression from AAV delivered promoter deletion constructs into the rat supraoptic nucleus in vivo. *PLOS One* **7**, e32085 (2012).

76. A. Cetin, S. Komai, M. Eliava, P. H. Seeburg, P. Osten, Stereotaxic gene delivery in the rodent brain. *Nat. Protoc.* **1**, 3166–3173 (2006).

Editor's Summary

Going Social

Oxytocin—a hormone that promotes mothering, trust, and social bonding in animals—seems a likely treatment for the social isolation of individuals on the autism spectrum, but tests in humans have generally proved disappointing. To delve deeper into how oxytocin affects autism symptoms, Peñagarikano *et al.* created a mouse mimic of one type of genetic autism, cortical dysplasia and focal epilepsy (CDFE) syndrome, by deleting the gene that is mutated in human patients. Unlike normal mouse-loving mice, CDFE mice were asocial, showing no preference for other mice over objects, but this deficit was reversed by giving them oxytocin. Further, revving up the sluggish production of their own oxytocin in the paraventricular nucleus in the hypothalamus also improved sociability. Most hopeful for patients, the authors found that giving young CDFE mice multiple doses of oxytocin just after birth produces a long-lasting improvement in oxytocin brain levels and sociability.